3D UNSTEADY VORTEX PANEL METHOD

WITH APPLICATIONS IN AERODYNAMICS

by

Pranav Prashant Ladkat
Spring 2015

A project submitted to the
Faculty of the Graduate School of
the University at Buffalo, State University of New York
in partial fulfilment of the requirements for the
degree of

Master of Science

Department of Mechanical and Aerospace Engineering

Pranav Prashant Ladkat

The project of Pranav Prashant Ladkat was reviewed by the following:

Dr. Iman Borazjani
Assistant Professor, Mechanical and Aerospace Department
Graduate Advisor

Dr. Cyrus K. Madnia
Professor, Mechanical and Aerospace Department
Committee Member

I dedicate my work to my family and friends. A special feeling of gratitude towards my loving parents, Prashant and Pratibha Ladkat for constant support and whose words of encouragement ring in my ears. My sisters Prachi who never left my side and is very special.

Acknowledgments

I wish to thank my committee members who were more than generous with their expertise and precious time. A special thanks to Dr. Iman Borazjani, my graduate advisor for his countless hours of reflecting, reading, encouraging, and most of all patience throughout the entire process. Thank you Dr. Cyrus Madnia, whose lecture notes helped me greatly in completing current work. I would also like to thank Dr. Mohsen Daghooghi who helped me in several ways during present study.

Table of Contents

List of Tables

List of Figures

List of Symbols

ϕ	Velocity Potential
σ	Source strength
μ	Doublet strength
$\mathbf{U}_\infty$	Free stream velocity
ρ	Density of the fluid
$\mathbf{u}$	Fluid velocity
p	Fluid pressure
Γ	Circulation
p_∞	Reference pressure
$\mathbf{v}_{ref}$	Reference velocity
$\mathbf{r}$	Position vector in spherical coordinates
ϕ_∞	Velocity potential due to free stream velocity
ϕ_i	Internal velocity potential
$\mathbf{v}_{apparent}$	Apparent or relative velocity between body and free stream velocity
Ω	Angular Velocity
γ	Strength of vortex element
$T.E.$	Trailing edge

$\mathbf{F}$	Force vector due to body
$\Delta\mathbf{F}$	Incremental force vector due to individual panel
v_l	Velocity in longitudinal direction of the panel
v_m	Velocity in transverse direction of the panel
$\mathbf{n}$	Normal vector of panel
$\mathbf{l}$	Longitudinal vector of panel
$\mathbf{m}$	Transverse vector of panel
$\mathbf{x}$	Coordinates of a point
B_k	Influence coefficient due to source panel
C_k	Influence coefficient due to doublet panel
RHS	Right hand side of the equation
Cp	Coefficient of pressure
Cl	Coefficient of lift
Cd	Coefficient of drag
A	Panel Area
FF	Farfield factor of the panel
m_a	Added mass

Abstract

In the present work, a first order vortex panel method is developed to study a potential flow around a body. A body is read in the form of a mesh file which discretizes the body into number of panels. Each panel is then assigned a constant strength source and doublet element. The aim of the developed code is to calculate strength of each source and doublet panel such that potential flow solution is solved with appropriate boundary conditions. Then the aerodynamic quantities (such as velocity, pressure and forces over the body) can be found from these source and doublet strengths. The developed code is then validated with several analytical and experimental results.

Chapter 1

Introduction

Computing flow around an object is one of the important application in an engineering. Aerodynamics is a sub-field of fluid dynamics which studies flow around an object. One of the key application in aerodynamics is to study flow over an airfoil which is widely used in aeroplane and helicopter wings, propellers, gas turbines, pumps, wind turbines etc. An optimization of an airfoil shape is an iterative process and we might need to test several different designs to come to a conclusion. Most accurate way to test a design is to conduct an experiment and test its output. However, it is extremely slow and costly process.

Panel Method is relatively old method and is in existence almost from the first appearance of computers. This method solves an inviscid flow around the body using singularity elements. Then aerodynamics coefficients can be computed in terms of those singularity elements. Panel Methods are now superseded by more advanced Computational Fluid Dynamics methods which makes use of Finite difference, Finite Volume and Finite Element methods to solve a flow field around a body. These methods are more sophisticated and can solve a more complex flow field taking into account for viscosity, turbulence and other physics. In CFD methods, the solution is calculated in the flow domain around the object and may extend to very large distance from the body to correctly apply boundary conditions. Hence huge amount of computational efforts are required to solve the flow field. Transient solution using these meth-

ods takes even more time. Hence even these methods tends to slow down the design and optimization process significantly.

In panel method, we only need to discretize the object's surface (unlike CFD methods where entire flow domain around an object needs to be discretized). Hence for a given problem, the number of unknowns are very small and thus the solution time is very small. This makes panel method an ideal method in the design and optimization process. However this is true only when the viscosity effects are less and there is no flow separation. This is usually true for an airfoil.

In the current work a low order, three dimensional unsteady panel method is developed making use of constant strength and doublet panels. And the objective is to compute the aerodynamic forces for various airfoil shapes. The fast solution time of the method makes it an ideal candidate to compute these forces and utilize them in real time.

Chapter 2 provides a brief theoretical background for the panel method and describes the flow equations which are being solved. Chapter 3 describes the solution algorithm of the vortex panel method, application of boundary conditions and other physical conditions to arrive at the unique solution. Chapter 4 describes implementation details of the method such as computation of geometric entities, calculations of velocity potential and flow velocities. Then Chapter 5 shows the results of the developed code and validates them by comparing with either analytical or experimental result. And chapter 6 finalizes the report with conclusion and future work.

Chapter 2

Potential Flow and its General Solution

2.1 Governing Equations of Fluid Flow

A fluid is composed of a large number of molecules in constant motion undergoing collisions with each other, and is therefore discontinuous or discrete at the most microscopic scales. There are two ways of deriving the equations that govern the motion of a fluid. One of these methods approaches the question from the molecular point of view. The alternative method used to derive the equations governing the motion of a fluid uses the continuum concept. In the continuum approach, individual molecules are ignored and it is assumed that the fluid consists of continuous matter. At each point of this continuous fluid there is supposed to be a unique value of the velocity, pressure, density, and other so-called field variables. The continuous matter is then required to obey the conservation laws of mass, momentum, and energy, which give rise to a set of differential equations governing the field variables. The solution to these differential equations then defines the variation of each field variable with space and time. The continuum hypothesis is valid for the flows under consideration in current work as region of interest are large enough and are sufficient for the explanation of macroscopic phenomena.

2.1.1 Conservation of Mass

Setting aside nuclear reactions mass is neither created nor destroyed. Thus, individual mass element-molecules, grains, fluid particles, etc. may be tracked within a flow field because they will not disappear and new elements will not spontaneously appear. Using Reynold's Transport Theorem the equation that expresses conservation of mass can be derived. The mass conservation equation is

$$\frac{\partial \rho}{\partial t} + \nabla.(\rho \mathbf{u}) = 0 \tag{2.1}$$

For incompressible fluid flows the density remains constant hence the mass conservation equation becomes

$$\nabla.\mathbf{u} = 0 \tag{2.2}$$

2.1.2 Navier-Stokes and Euler Equations

The equation of momentum conservation together with the constitutive relation for a Newtonian fluid yield the famous Navier-Stokes equations, which are the principal conditions to be satisfied by a fluid as it flows. For the Newtonian fluid with constant density, Navier-Stokes equation reduces to

$$\rho \left(\frac{\partial \mathbf{u}}{\partial t} + \nabla.\mathbf{u} \right) = -\nabla p + \mu \Delta \mathbf{u} \tag{2.3}$$

When the convective effects are dominant in the flow compared to viscous effects, the viscosity term can be neglected. When viscous term in the (2.3) is neglected, resultant equation is called the Euler equation which governs inviscid flow.

$$\frac{\partial \mathbf{u}}{\partial t} + \nabla.\mathbf{u} = -\frac{1}{\rho}\nabla p \tag{2.4}$$

Equations (2.2) and (2.4) are sufficient to establish the velocity and the pressure in the flow independent of any temperature distribution that may exist. Within macroscopic length scales, the proper boundary condition to be satisfied

by the velocity is the no-slip boundary condition. It is not possible to satisfy this boundary condition with the Euler equations. The reason lies in the fact that the Euler equations are one order lower than the Navier-Stokes equations because the viscous terms are absent in the former equations. Thus the true boundary condition must be relaxed somehow under the approximation of negligible viscous effects. Since it is primarily viscous effects that prohibit a fluid from slipping along a solid boundary, the condition of no tangential slip at boundaries is relaxed. That is, the condition of no normal velocity at a solid boundary is retained but the condition of no tangential velocity is dropped.

$$\mathbf{u}.\mathbf{n} = 0 \tag{2.5}$$

2.1.3 Kelvin's Theorem

This theorem states that for an inviscid fluid in which the density is constant, or in which the pressure depends on the density alone, and for which any body forces that exist are conservative, the vorticity of each fluid particle will be preserved. Kelvin theorem can be derived from Navier-Stokes equations and are represented by

$$\frac{D\Gamma}{Dt} = 0 \tag{2.6}$$

where, Γ is the circulation.

2.1.4 Velocity Potential and Laplace Equation

If the flow of an ideal fluid about a body originates in an irrotational flow, such as a uniform flow, for example, then Kelvins theorem (2.6) guarantees that the flow will remain irrotational even near the body. That is, the vorticity vector ω will be zero everywhere in the fluid. since $\nabla \times \nabla\phi = 0$ for any scalar function ϕ, the condition of irrotationality will be satisfied identically by choosing

$$\mathbf{u} = \nabla\phi \tag{2.7}$$

The function ϕ is called the velocity potential. When (2.7) is substituted in continuity equation (2.2) gives

$$\nabla^2\phi = 0 \tag{2.8}$$

Thus by solving equation (2.8) and utilizing equation (2.2), the velocity field may be established without directly using the equations of motion.

2.1.5 Bernoulli's Equation for Pressure

For an inviscid fluid in which any body forces are conservative and either the flow is steady or it is irrotational, the equations of momentum conservation may be integrated to yield a single scalar equation called the Bernoulli equation.

$$\frac{\partial\phi}{\partial t} + \frac{p}{\rho} + \frac{1}{2}\nabla\phi.\nabla\phi = C(t) \tag{2.9}$$

A more useful form of Bernoulli equation is obtained by comparing the quantities on the left hand side of equation (2.9) at two points in the fluid. First is an arbitrary point, and second is a reference point at infinity. Then the equation becomes

$$\frac{p_\infty - p}{\rho} = \frac{\partial\phi}{\partial t} + \frac{u^2}{2} \tag{2.10}$$

The coefficient of pressure can be found by

$$C_p = 1 - \frac{1}{u_{ref}^2}\left(\mathbf{u}^2 + 2\frac{\partial\phi}{\partial t}\right) \tag{2.11}$$

2.2 General Solution of Potential Flow Problem

2.2.1 Problem Statement

When the flow in the fluid region is considered to be incompressible and irrotational then the continuity equation reduces to

$$\nabla^2\phi = 0$$

given by equation (2.8). For a submerged body in the fluid, the velocity component normal to the bodys surface and to other solid boundaries must be zero, and in a body-fixed coordinate system:

$$\nabla\phi.\mathbf{n} = 0 \tag{2.12}$$

Here $\mathbf{n}$ is a vector normal to the bodys surface, and $\nabla\phi$ is measured in a frame of reference attached to the body. Also, the disturbance created by the motion should decay far ($r \to \infty$) from the body:

$$\lim_{x\to\infty}(\nabla\phi - \mathbf{v}) = 0 \tag{2.13}$$

where $\mathbf{r} = (x, y, z)$ and $\mathbf{v}$ is relative velocity between the fluid and the body.

2.2.2 General Solution

General solution based on Green's Identity is derived in [1], which gives the potential at any point P outside the body is

$$\phi(P) = -\frac{1}{4\pi}\int_{S_B}\left[\sigma\left(\frac{1}{\mathbf{r}}\right) - \mu\frac{\partial}{\partial\mathbf{n}}\left(\frac{1}{\mathbf{r}}\right)\right]dS + \frac{1}{4\pi}\int_{S_W}\left[\mu\frac{\partial}{\partial\mathbf{n}}\left(\frac{1}{\mathbf{r}}\right)\right]dS + \phi_\infty(P) \tag{2.14}$$

where $\phi(P)$ is potential at point P, S_B represents boundary surface, S_W represents wake surface. σ is called *source* element and μ is called *doublet* element, $\mathbf{r}$ is position vector in spherical coordinates. To find the velocity potential, the strength of the distribution of doublet and sources on the surface must be deter-

mined. Equation (2.14) does not specify a unique combination of sources and doublets for a particular problem and a choice must be made in this matter. The common practice is to determine the source strength [4] by

$$\sigma = -\mathbf{n}.V_{apparent} \tag{2.15}$$

where

$$V_{apparent} = (\mathbf{V}_{linear} + \Omega \times \mathbf{r}) - \mathbf{V}_{free\_stream\_velocity} \tag{2.16}$$

and $\mathbf{V}_{linear}$ and Ω are the linear and angular velocity of the body. Negative sign is used by assuming that velocity of body is in opposite direction to that of free stream velocity.

2.2.3 Basic Solution: Source element

One of the two basic solutions presented in Equation (2.14) is the source/sink. When the strength of this element (σ) is positive, it is called source and if negative, it is called sink. The potential at a point $P(x, y, z)$ due to point source element located at (x_0, y_0, z_0) is

$$\begin{aligned} \phi(P(x,y,z)) &= -\frac{\sigma}{4\pi|\mathbf{r}-\mathbf{r}_0|} && \text{(spherical coordinates)} \\ &= \frac{-\sigma}{4\pi\sqrt{(x-x_0)^2+(y-y_0)^2+(z-z_0)^2}} && \text{(cartesian coordinates)} \end{aligned} \tag{2.17}$$

It is possible to distribute basic solutions over a surface, usually called as Panels. Hence the potential at a point $P(x, y, z)$ due to the surface distribution of source element can be achieved by integrating equation (2.17),

$$\phi(P(x,y,z)) = \frac{-1}{4\pi}\int_S \frac{-\sigma(x_0,y_0,z_0)}{\sqrt{(x-x_0)^2+(y-y_0)^2+(z-z_0)^2}}\, dS \tag{2.18}$$

The velocity field due to this element can be found by differentiating equa-

tion (2.18),

$$(u, v, w) = \left(\frac{\partial \phi}{\partial x}, \frac{\partial \phi}{\partial y}, \frac{\partial \phi}{\partial z}\right) \tag{2.19}$$

The figure (2.1) shows the velocity field due to a single source panel. The velocity vectors in the figure are normalized for better visualization, however the velocity decays in the radial direction with the rate of $1/r^2$. The numerical formulae for computing the velocity field is discussed in section 4.7.1

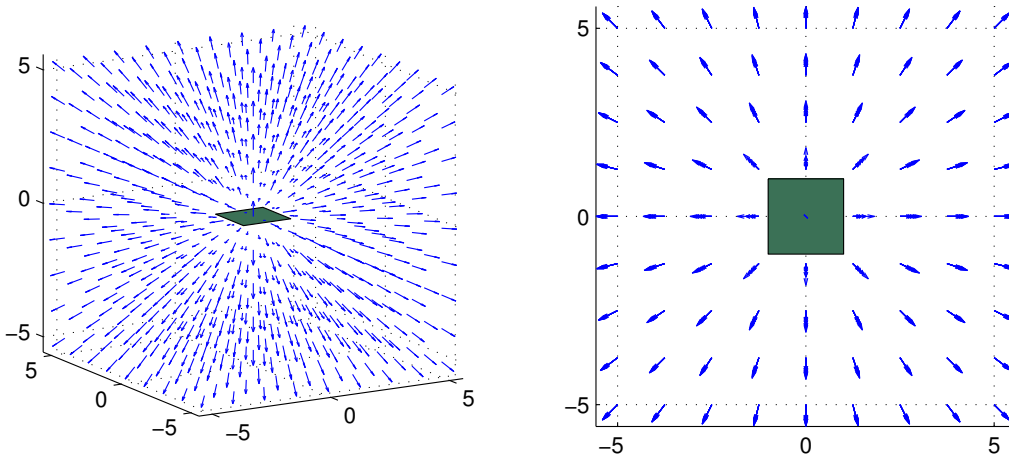

Figure 2.1. Velocity vectors due to single Source panel. Velocity vectors are normalized.

2.2.4 Basic Solution: Doublet Element

The second basic solution used in the equation (2.14) is called doublet. The potential due to doublet element in spherical coordinates is given by

$$\phi = \frac{\mu}{4\pi}\mathbf{n}.\nabla\left(\frac{1}{|\mathbf{r} - \mathbf{r}_0|}\right) \tag{2.20}$$

Taking the dot product of normal and gradient of position vector, the resulting differential in x direction is

$$\phi(x, y, z) = \frac{-\mu}{4\pi}(x - x_0)\left[(x - x_0)^2 + (y - y_0)^2 + (z - z_0)^2\right]^{-3/2} \tag{2.21}$$

The result of differential in y direction in

$$\phi(x,y,z) = \frac{-\mu}{4\pi}(y-y_0)\left[(x-x_0)^2+(y-y_0)^2+(z-z_0)^2\right]^{-3/2} \tag{2.22}$$

The result of differential in z direction in

$$\phi(x,y,z) = \frac{-\mu}{4\pi}(z-z_0)\left[(x-x_0)^2+(y-y_0)^2+(z-z_0)^2\right]^{-3/2} \tag{2.23}$$

Usually, the point $P(x,y,z)$ is transformed into panel's local coordinates hence only one of the component from above needs to be evaluated. Similar to source element, doublet element can be distributed over a surface and potential due to surface doublet can be obtained by integrating point doublet formula. The z-component of the such doublet panel will be

$$\phi(x,y,z) = \frac{-1}{4\pi}\int_S \frac{\mu(x_0,y_0,z_0).(z-z_0)}{[(x-x_0)^2+(y-y_0)^2+(z-z_0)^2]^{3/2}}\,dS \tag{2.24}$$

The velocity due to doublet panel can be obtained by differentiating ϕ as in equation (2.19). The figure (2.2) shows the velocity due to doublet pointing in the normal direction to the panel. The numerical formulae for computing velocity due to doublet is discussed in section 4.7.1

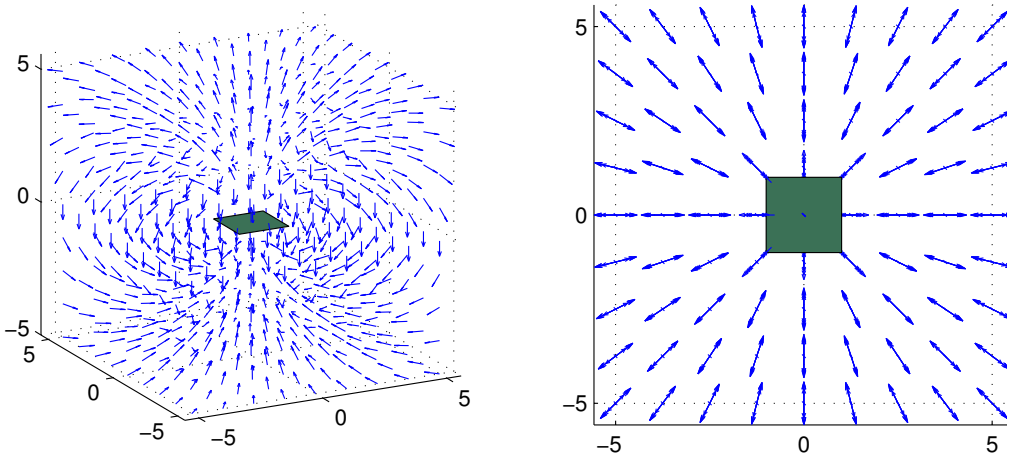

Figure 2.2. Velocity vectors due to Doublet panel. Velocity vectors are normalized.

Chapter 3

Vortex Panel Method

Panel Method solves the equation (2.14) numerically by distributing singularity elements on the surface over which flow field needs to be computed. To do this, the surface is discretized into smaller surface elements (panels). Every panel is assigned with one or more singularity element strengths. In the present work *Constant Strength Source and Doublet Panel* is implemented. Hence every panel will have a unique source and doublet strength values which will be constant. The figure (3.1) shows an example of discretization of a surface which is generally used in Panel Method.

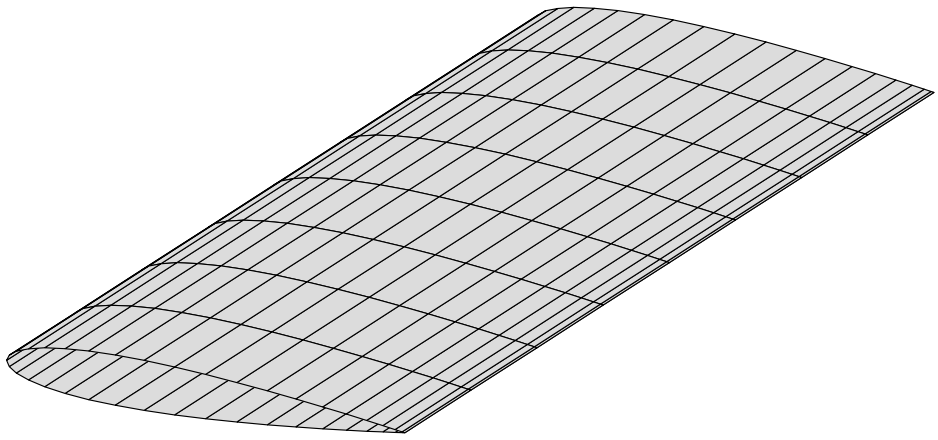

Figure 3.1. Example of discretized surface of NACA0012 airfoil

Since the solution is now reduced to finding the strength of the singularity elements distributed on the bodys surface this approach seems to be more eco-

nomical, from the computational point of view, than methods that solve for the flow field in the whole fluid volume (e.g.,finite difference methods). Of course this comparison holds for inviscid incompressible flows only.

Consider a body with known boundaries S_B, submerged in a potential flow as shown in figure (3.1). The flow of interest is in the outer region V where the incompressible, irrotational continuity equation, in terms of the total potential is given by equation (2.8). Using the Green's identity, the general solution of the equation (2.8) can be constructed by a sum of source σ and doublet μ distributions placed on the boundary S_B and is given by equation (2.14). The boundary conditions of zero flow normal to the surface must be applied to yield the solution.

In the general case of three-dimensional flows, specifying the boundary conditions alone will not immediately yield a unique solution because of two problems. First, a decision has to be made in regard to the right combination of source and doublet distributions. Usually the strength of the source element is set to the local kinematic velocity as described by equation (2.15). This equation also takes into account the unsteady boundary conditions. This formulation is used in PMARC [4] code. Second, some physical considerations need to be introduced to fix the amount of circulation around the surface S_B. These considerations deal mainly with the modeling of the wakes and fixing the wake shedding lines and their initial orientation and geometry. This is discussed in section 3.4

3.1 Dirichlet Boundary Condition

The boundary condition for equation (2.8) can directly specify a zero normal velocity component $\partial\phi/\partial n = 0$ on the surface S_B, in which case this direct formulation is called the *Neumann problem*. It is also possible to specify ϕ on the boundary, so that indirectly the zero normal flow condition will be met, and this indirect formulation is called the *Dirichlet problem*. A combination of the above boundary conditions is possible, too, and this is called a *Mixed Boundary Condition problem*. The current work uses *Dirichlet boundary conditions*.

If for an enclosed boundary (e.g., S_B) $\partial\phi/\partial n = 0$, as required by the bound-

ary condition in equation (2.5), then the potential inside the body (without internal singularities) will not change[5], that is,

$$\phi_i = constant \tag{3.1}$$

For Dirichlet boundary condition, the perturbation potential ϕ has to be specified everywhere on S_B. Equation (2.14) does this exactly, and by distributing the singularity elements on the surface, and placing the point (x, y, z) inside the surface S_B, the inner potential ϕ_i in terms of the surface singularity distributions is obtained:

$$\begin{aligned} \phi_i(x,y,z) &= \frac{1}{4\pi}\int_{body+wake} \mu \frac{\partial}{\partial n}\left(\frac{1}{\mathbf{r}}\right)\, dS - \frac{1}{4\pi}\int_{body} \sigma\left(\frac{1}{\mathbf{r}}\right)\, dS + \phi_\infty \\ &= constant \end{aligned} \tag{3.2}$$

The inner potential constant can be set to $\phi_i = \phi_\infty$, then equation (3.2) reduces to simpler form:

$$\frac{1}{4\pi}\int_{body+wake} \mu \frac{\partial}{\partial n}\left(\frac{1}{r}\right)\, dS - \frac{1}{4\pi}\int_{body} \sigma\left(\frac{1}{r}\right)\, dS + \phi_\infty = 0 \tag{3.3}$$

This equation is used in the current work. Due to utilization of Dirichlet boundary conditions, only thick bodies can be simulated by the current method.

3.2 Kutta Condition

The above mathematical formulation, even after selecting a desirable combination of sources and doublets, and after fulfilling the boundary conditions on the surface S_B, is not unique. For describing the flow over thick bodies without lift, the source distribution is sufficient, but for the lifting cases the amount of the circulation is not uniquely defined. The Kutta-condition states that "A body with a sharp trailing edge which is moving through a fluid will create about itself a circulation of sufficient strength to hold the rear stagnation point at the trailing edge". For the wing to have circulation Γ at a spanwise location, a discontinuity

in the velocity potential near the trailing edge must exist:

$$\phi_2 - \phi_1 = \Gamma \tag{3.4}$$

Where ϕ_1 is the potential under the thin wake and ϕ_2 is above the wake. Now to get a unique solution for the problem, additional physical considerations can be established in relation to a wake model. This model has to specify two additional conditions:

1. To set the wake strength at the trailing edge
2. To set its shape and location

The strength of the wake at trailing edge can be set by applying the two-dimensional Kutta condition along the three-dimensional trailing edge such that

$$\gamma_{T.E.} = 0 \tag{3.5}$$

where, $\gamma_{T.E.}$ is the strength of the vortex element located at the trailing edge. The vortex distribution can be replaced by equivalent doublet distribution such that

$$\gamma(x) = -\nabla\mu(x) \tag{3.6}$$

Therefore, the condition in equation (3.5) can be rewritten for the trailing-edge line, such that μ is constant in the wake (μ_w) and equals the value at the trailing-edge ($\mu_{T.E.}$), that is,

$$\mu_{T.E.} = constant \equiv \mu_W \tag{3.7}$$

$$\text{or,} \qquad \mu_U - \mu_L = \mu_W \tag{3.8}$$

where, μ_U and μ_L are the corresponding upper and lower surface doublet strengths at the trailing edge.

The second condition to define wake shape and location which needs to be satisfied and it is discussed in section 3.4

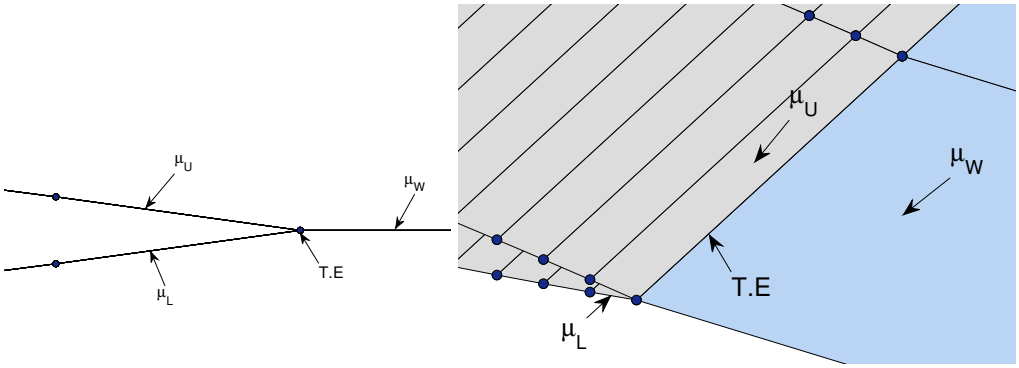

Figure 3.2. Implementation of Kutta Condition

3.3 Reducing Problem to a Set of Algebraic Equations

At this point it is assumed that the problem is unique and that a combination of source/doublet distributions has been selected along with a wake model and the Kutta condition. The boundary condition will be specified at each of these elements at a collocation point which is usually a centroid of the center. If we discretize surface into N panels, we can rewrite (3.3) for each collocation point in following form:

$$\begin{aligned} 0 = &\sum_{k=1}^{N} \frac{1}{4\pi} \int_{bodypanel} \mu \mathbf{n}.\nabla \left(\frac{1}{r}\right)\ dS + \sum_{l=1}^{N_W} \frac{1}{4\pi} \int_{wakepanel} \mu \mathbf{n}.\nabla \left(\frac{1}{r}\right)\ dS \\ &- \sum_{k=1}^{N} \frac{1}{4\pi} \int_{bodypanel} \sigma \left(\frac{1}{r}\right)\ dS \end{aligned} \tag{3.9}$$

That is, for each collocation point P the summation of the influences of all k body panels and l wake panels is needed. The integration in equation (3.9) is limited now to each individual panel element representing the influence of this panel on point P. For a unit singularity element (σ or μ), this influence depends on the panels geometry only, hence are usually calculated prior to calculations. The influence of the doublet panel l at point P is

$$\frac{1}{4\pi} \int_{l} \frac{\partial}{\partial n} \left(\frac{1}{r}\right)\ dS \equiv C_k \tag{3.10}$$

and for a constant strength source element:

$$-\frac{1}{4\pi}\int_l \left(\frac{1}{r}\right)\, dS \equiv B_k \tag{3.11}$$

These integrals are the functions of the panel coordinates and point P only and can be included in a separate functions. After computing the influence of each panel on each other panel, equation (3.9) for each point P insides the body becomes

$$\sum_{k=1}^{N} C_k\mu_k + \sum_{l=1}^{N_w} C_l\mu_l + \sum_{k=1}^{N} B_k\sigma_k = 0 \tag{3.12}$$

This equation is the numerical equivalent of the boundary condition. If the strengths of the sources are selected according to equation (2.15), then third term in equation (3.12) for each panel is known, hence can be moved to the right-hand side of the equation. Also, by using the Kutta condition, the wake doublets can be expressed in terms of the unknown surface doublets μ_k. For example, two of the trailing edge (T.E.) doublets μ_u and μ_l are related to the corresponding wake doublet μ_w. Here, u, l, w are arbitrary counters where u denotes the upper panel, l denotes the lower panel and w denotes the wake panel. The μ_w can be expressed in terms of μ_u and μ_l as

$$\mu_w = \mu_u - \mu_l$$

and the influence of the wake panel becomes

$$C_w\mu_w = C_w(\mu_u - \mu_l)$$

This algebraic relation can be substituted into the C_k coefficients of the unknown surface doublet such that

$$\begin{aligned} A_k &= C_k && \text{if panel is not at T.E} \\ A_k &= C_k \pm C_w && \text{if panel is at T.E} \end{aligned}$$

where $\pm$ depends whether the panel is at the upper or lower side of the T.E.

Hence, for each collocation point P, a linear algebraic equation containing N unknown singularity variables μ_k can be derived as

$$\sum_{k=1}^{N} A_k \mu_k = -\sum_{k=1}^{N} B_k \sigma_k \tag{3.13}$$

Evaluating equation (3.13) for each of the N collocation points results in N equations with N unknown μ_k in the following form:

$$\begin{bmatrix} a_{1,1} & a_{1,2}, & ... & a_{1,N} \\ a_{2,1} & a_{2,2}, & ... & a_{2,N} \\ \vdots & \vdots & ... & \vdots \\ a_{N,1} & a_{N,2}, & ... & a_{N,N} \end{bmatrix} \begin{bmatrix} \mu_1 \\ \mu_2 \\ \vdots \\ \mu_N \end{bmatrix} = - \begin{bmatrix} b_{1,1} & b_{1,2}, & ... & b_{1,N} \\ b_{2,1} & b_{2,2}, & ... & b_{2,N} \\ \vdots & \vdots & ... & \vdots \\ b_{N,1} & b_{N,2}, & ... & b_{N,N} \end{bmatrix} \begin{bmatrix} \sigma_1 \\ \sigma_2 \\ \vdots \\ \sigma_N \end{bmatrix} \tag{3.14}$$

The σ is already known, hence right hand side of the equation (3.14) can be computed and rewritten as:

$$\begin{bmatrix} a_{1,1} & a_{1,2}, & ... & a_{1,N} \\ a_{2,1} & a_{2,2}, & ... & a_{2,N} \\ \vdots & \vdots & ... & \vdots \\ a_{N,1} & a_{N,2}, & ... & a_{N,N} \end{bmatrix} \begin{bmatrix} \mu_1 \\ \mu_2 \\ \vdots \\ \mu_N \end{bmatrix} = \begin{bmatrix} RHS_1 \\ RHS_2 \\ \vdots \\ RHS_N \end{bmatrix} \tag{3.15}$$

The equation (3.15) is solved for the unknown μ using any numerical method for solving dense linear system of equations. Once the doublet and source strength for all panels are known, the surface velocity and aerodynamics loads can be computed. This is described in section 3.5

3.4 Wake Modeling: Force Free Wake

In three dimensions, the wake influence is more dominant than in two dimensions and its geometry clearly affects the solution. Hence the wake needs to be modelled for more correct solution. To distinguish between the models for bound circulation (which generate the lift) and the circulation shed into the wake, it is logical to assume that the wake should not produce lift, since it is

not a solid surface. When the wake is modeled by vortex elements, the Kutta Joukowski theorem for lift states that

$$\Delta \mathbf{F} = \rho \mathbf{V} \times \gamma$$

$\mathbf{F}$ is the force generated by the vortex sheet γ. For three dimensions, $\Delta \mathbf{F} = 0$ only if the local flow is parallel to γ. Hence the condition for the wake geometry is

$$\mathbf{V} \times \gamma_W = 0$$

or

$$\gamma_W || \mathbf{V} \tag{3.16}$$

that is vorticity vector is parallel to the local velocity vector. Using equation (3.6), an equivalent wake representation can be obtained:

$$\mathbf{V} \times \nabla \mu_W = 0$$

So the condition for the wake panels in terms of doublets, is

$$\mu_w = constant \tag{3.17}$$

and the boundaries of these elements (which are really the vortex lines) should be parallel to the local streamlines. This condition given by equation (3.16) is difficult to satisfy exactly since the wake location is not known in advance.

In the current work, the wake is modelled using *Time Stepping Method* or also known as *Force Free Wake*. The equation (3.17) states that the strength should be constant and hence the shedded wake will retain its strength in the time. For the first time step, the system of equations will be the same as in (3.15). After computing the solution of (3.15), the strength of the wake panels μ_W can be calculated by using the relation (3.8). Once we have the strength of all singular elements, the total velocity at nodes comprising wake panels can be found out (except for the nodes matching the trailing edge). The total velocity at a point P

can be obtained by

$$\mathbf{V}_{total} = \sum_{k=1}^{N_{body}} \mathbf{v}_{\sigma} + \sum_{k=1}^{N_{body}} \mathbf{v}_{\mu_b} + \sum_{l=1}^{N_{wake}} \mathbf{v}_{\mu_w} \tag{3.18}$$

where $\mathbf{V}_{\sigma_b}$ and $\mathbf{V}_{\mu_b}$ is the velocity due to source and doublet strengths of body panels and $\mathbf{V}_{\sigma_w}$ is the velocity due to doublet wake panels. And these points (except on trailing edge) are convected using

$$\Delta\mathbf{x} = \mathbf{V}_{total}\Delta t \tag{3.19}$$

where $\Delta\mathbf{x}$ is the change in position of a point and Δt is the solution time step. The nodes on the trailing edge are convected using

$$\Delta\mathbf{x} = \alpha\mathbf{V}_{apparent}\Delta t \tag{3.20}$$

where, the $\mathbf{V}_{apparent}$ is given by (2.16). And α is usually taken from a range of 0.2 to 0.3. As the wake is convected, a new row of wake panels are created with the nodes on trailing edge from previous time-step and current nodes on the trailing edge. The strength of the wake panels at the previous time steps is

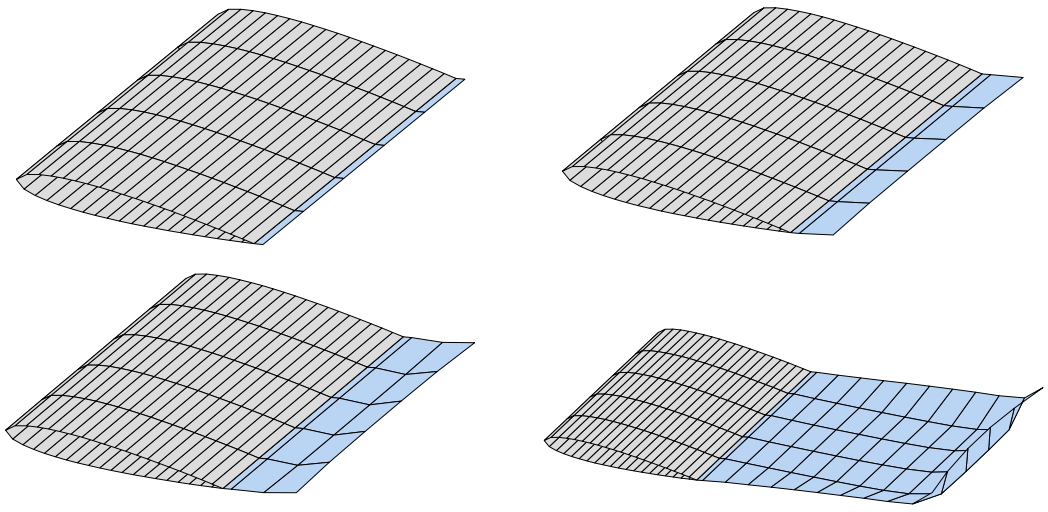

Figure 3.3. Time stepping procedure of wake shedding. The figure shows the wake at time step 1, 2, 3 and 11.

retained for all future time steps. Hence the equation (3.12) takes the form

$$\sum_{k=1}^{N} C_k \mu_k + \sum_{k=1}^{N} B_k \sigma_k + \sum_{l=1}^{N_{T.E}} C_l \mu_l + \sum_{m=1}^{N_W - N_{T.E}} C_m \mu_m = 0 \tag{3.21}$$

here, wake panels are classified into two separate summations. The counter l scans for wake panels which are adjacent to trailing edge and its wake doublet strength is unknown. The counter m scans for rest of the wake panels which are shed in previous time steps and its doublet strength is known. As the strength of σ_k and μ_m is alreadky known, this can be taken to right hand side, hence the (3.22) can be written as:

$$\sum_{k=1}^{N} C_k \mu_k + \sum_{l=1}^{N_{T.E}} C_l \mu_l = -\sum_{k=1}^{N} B_k \sigma_k - \sum_{m=1}^{N_W - N_{T.E}} C_m \mu_m \tag{3.22}$$

which again reduces to similar equation (3.15) with RHS term having extra contribution from wake panels (except those are attached to trailing edge, where Kutta condition is applied).

3.5 Calculation of Aerodynamic Loads

Once Equation (3.15) is solved the unknown singularity values are obtained. Then surface velocity is computed now in terms of the panel local coordinates (l, m, n) as shown in Figure (3.4). The two tangential perturbation velocity components are

$$\begin{aligned} v_l &= -\frac{\partial \mu}{\partial l} + V_{apparent_l} \\ v_m &= -\frac{\partial \mu}{\partial m} + V_{apparent_m} \end{aligned} \tag{3.23}$$

where the differentiation is done numerically using the values on the neighbour panels. The normal component of the velocity on the boundary will be zero. Note that the $V_{apparent}$ is also transformed to panel local coordinates.

Once the surface velocity is calculated, we can compute the pressure coeffi-

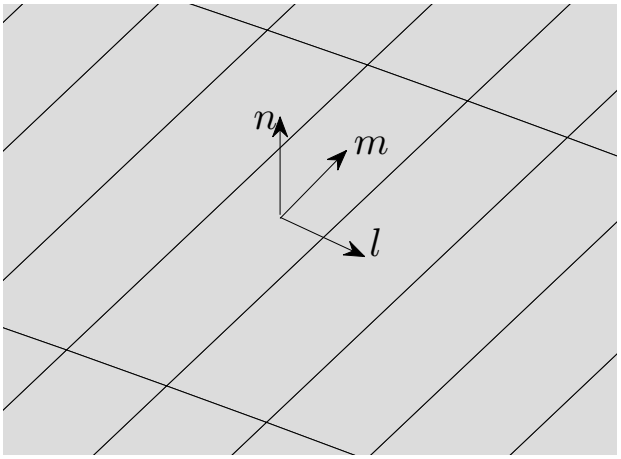

Figure 3.4. Panel local coordinate system

cient from equation (2.11)

$$C_{p_{panel}} = 1 - \frac{1}{u_{ref}^2}\left(\mathbf{u}_{panel}^2 + 2\frac{\partial \phi}{\partial t}\right)$$

where $\mathbf{u}_{panel}$ is $(v_l, v_m, 0)$ in panel local coordinates and $\frac{\partial \phi}{\partial t}$ is $\frac{\partial \mu}{\partial t}$.

After calculating the coefficient of pressure, the panel contribution to the fluid dynamic loads is calculated using

$$\Delta \mathbf{F}_{panel} = \frac{1}{2}\,\rho\, v_{ref}^2\, C_{p_{panel}}\, \mathbf{n}\, dA \tag{3.24}$$

where $\frac{1}{2}\,\rho\, v_{ref}^2$ is the dynamic pressure, $\mathbf{n}$ is panel normal and dA is the panel area. Forces from each panel can be summed up to compute total aerodynamics forces on the body.

3.6 Solution Algorithm

We can sum up the overall algorithm for vortex panel method as

1. Define Geometry: Read the input geometry in mesh format
2. Flight Path Information: Specify the momentary body's kinematic velocity and orientation. Also specify the free stream velocity. This can be different

at different time step to account unsteady behaviour.

3. Calculation of Influence Coefficient: Calculate the panel's geometric entities and compute influence coefficient used in forming the matrix
4. Calculation of Momentary RHS: With the given body source and wake doublet strength, right hand side vector can be computed.
5. Solution of the Matrix: The system of equations are solved in this step giving the solution of unknown body's doublet strengths
6. Calculation of Velocity, Pressure and Body Forces
7. Wake Rollup: The wake is convected with local kinematic velocity
8. Iterate from step 2 to 7 until the final time

The solution algorithm is summarized in the figure (3.5)

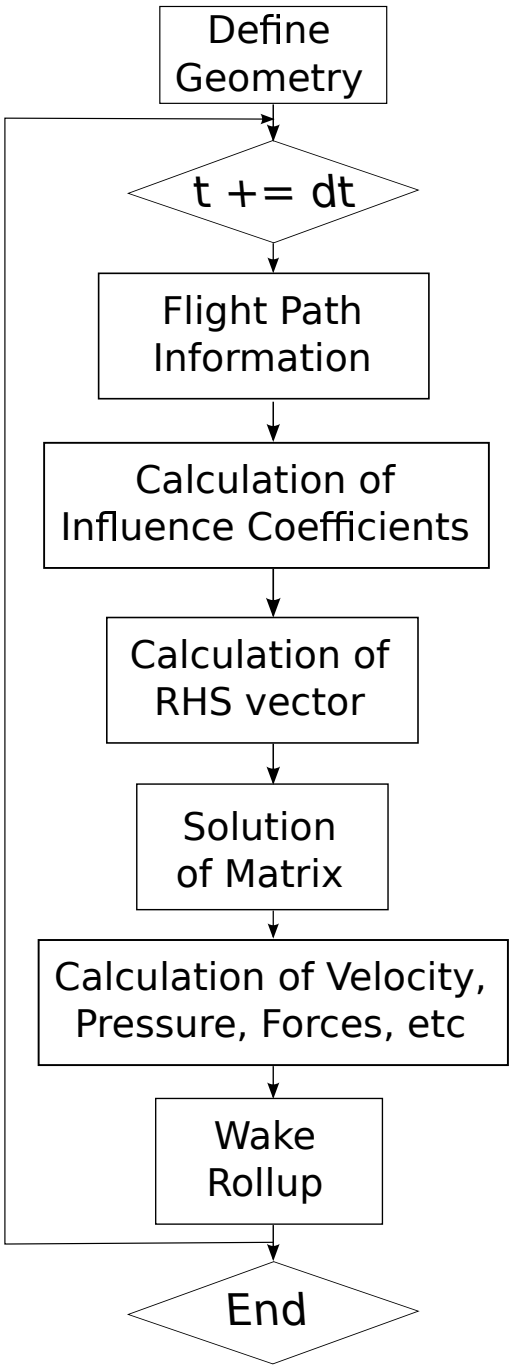

Figure 3.5. Schematic flowchart for the numerical solution of unsteady panel method

Chapter 4

Implementation Details of Vortex Panel Method

The overall algorithm of the Vortex Panel Method is discussed in the previous chapter. This chapter provides most of the implementation details which are requited to get correct solution.

4.1 Collocation Point

The equation (2.8) is solved at the collocation point of each panel, and boundary conditions are also satisfied at these points. Hence it is necessary to compute the collocation point for each panel. The collocation point is usually taken as the centroid of the panel.

$$\mathbf{x}_{cp} = \frac{1}{n}\left(\sum_{i=1}^{n} \mathbf{x}_i\right) \tag{4.1}$$

where, n in the number of nodes for each panel, $\mathbf{x} = (x, y, z)$ and subscript cp denotes collocation point. Equation (4.1) gives the collocation point for quadrilateral faces as:

$$\mathbf{x}_{quad}(x, y, z) = \left(\frac{x_1 + x_2 + x_3 + x_4}{4}, \frac{y_1 + y_2 + y_3 + y_4}{4}, \frac{z_1 + z_2 + z_3 + z_4}{4}\right)$$

4.2 Panel Local Coordinates

The calculation of the influence coefficients, and velocity computation is done in panel's local coordinates to efficiently compute the integrals in the influence coefficients formulas. For this purpose, local panel coordinates are usually pre computed and used in later calculations. In current work, panel points are stored in the anti-clockwise sense so that computed normal always points in the outward direction and also other panel coordinates will be defined consistently. We will call three coordinates as Normal vector, Longitudinal Vector and Transverse Vector.

4.2.1 Normal Vector

The panel normal vector is computed by taking the cross product of the two vectors which are on the panel's plane. For a quadrilateral panel, these two vectors are defined as the vector pointing from one panel corner to opposite corner. And for a triangular panel, two edges of the panels are taken as shown in the figure (4.2). Then normal vector is computed from

$$\mathbf{n} = \frac{\mathbf{AB} \times \mathbf{CD}}{||\mathbf{AB} \times \mathbf{CD}||} \tag{4.2}$$

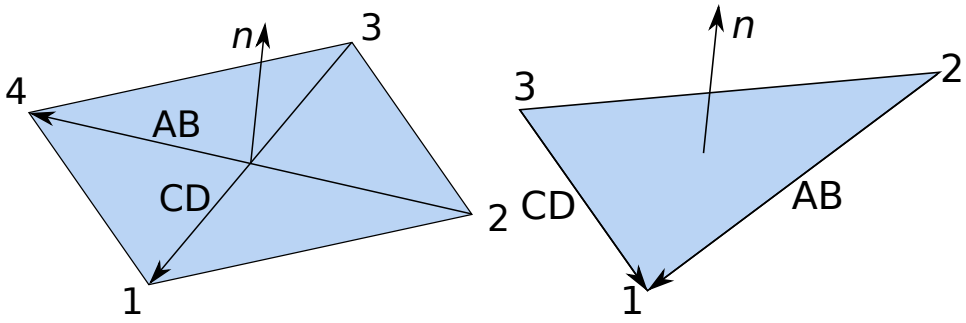

Figure 4.1. Defining the panel normal vector

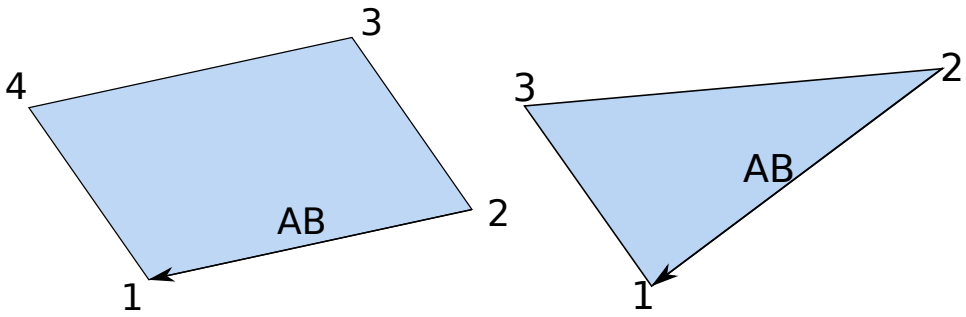

Figure 4.2. Defining the panel longitudinal vector

4.2.2 Longitudinal Vector

Longitudinal vector is taken as any edge vector. In the current work, the normalized vector pointing from point 2 to 1 is taken as longitudinal vector. Hence the longitudinal vector is

$$\mathbf{l} = \frac{\mathbf{AB}}{||\mathbf{AB}||} \tag{4.3}$$

4.2.3 Transverse Vector

Transverse vector defines the third panel coordinate and it should be perpendicular to normal vector and longitudinal vector. Hence the transverse vector is computed by taking cross product of normal vector and longitudinal vector.

$$\mathbf{m} = \mathbf{n} \times \mathbf{l} \tag{4.4}$$

m will already be normalized.

4.2.4 Panel's Transformation Matrix

The panel's local coordinate vectors can be written in the form of a matrix which can be used later in the calculations. The transformation matrix will be

$$[T] = \begin{bmatrix} l_x & l_y & l_z \\ m_x & m_y & m_z \\ n_x & n_y & n_z \end{bmatrix} \tag{4.5}$$

4.3 Far-field Factor of a panel

While calculating influence coefficients and disturbance velocity at a point, entire panel geometry is considered in the integral formulas. When the point of influence is far enough from the panel, it can be approximated as a point source. This reduces the amount of calculations without introducing significant error. The farfield factor is defined in terms of the maximum diagonal of the panel in case of quadrilateral panel or maximum edge length of the triangular panel. Lets denote the maximum diagonal (or edge) by d. Then the Farfield factor can be set to

$$FF_{panel} = \alpha \; d_{panel} \tag{4.6}$$

where α is generally taken as 3-5. In the current work, it is taken as 10.

4.4 Transform a Point in Panel's Local Coordinates

As mentioned earlier, all calculations of influence coefficients and disturbance velocity is done in panel's local coordinates. Point $\mathbf{x}$ can be converted to panel's local coordinates by

$$\begin{aligned} \mathbf{r} &= \mathbf{x} - \mathbf{x}_{cp} \\ \mathbf{x}_{local} &= \mathbf{r}\,[T] \end{aligned} \tag{4.7}$$

where, $\mathbf{x}_{local}$ is transformed point, $\mathbf{x}_{cp}$ is panel's collocation point, $\mathbf{r}$ is a vector pointing from $\mathbf{x}$ to $\mathbf{x}_{cp}$. Here, $\mathbf{x}_{local}$, $\mathbf{x}_{cp}$ and $\mathbf{r}$ are 3 dimensional space vectors (x, y, z). This can easily put in a function which takes panel id and $\mathbf{x}$ as input and return $\mathbf{x}_{local}$.

4.5 Transformation of Vector

We also need to transform a vector in panel's coordinates for some calculations such as transform free stream velocity in panel's coordinates and add it with disturbance velocity to get the total surface velocity at collocation point of a

panel. This is similar to equation (4.7) except we do not need to compute **r** and directly multiple vector by panel's transformation matrix (4.5).

$$\mathbf{Vec}_{local} = \mathbf{Vec}\ [T] \tag{4.8}$$

And to transform a local vector (from panel's local coordinates) back to global vector, we can multiply local vector with the transpose of the transformation matrix. This is mostly required for flow visualization after the solution is computed.

$$\mathbf{Vec} = \mathbf{Vec}_{local}\ [T]^{transpose} \tag{4.9}$$

4.6 Calculations of Influence Coefficients

The calculations of influence coefficient is the most important and compute intensive part of this method. In the current work, a constant strength source and doublet element is used, i.e., σ and μ both are some constant for a given panel. The equations (3.10) and (3.11) gives the influence due to a unit strength doublet and source panel, respectively. The calculations of the integrals in those equations can be done numerically but the analytical integrals as calculated by Hess and Smith [2] are used.

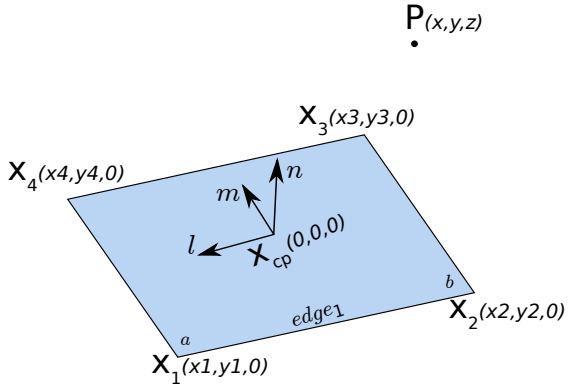

Figure 4.3. Notations used in influence coefficient calculations. All coordinates are in panel local coordinates

4.6.1 Influence Coefficient due to Source Panel

The integral in equation (2.18) is approximated to get the influence coefficient due to unit source strength source panel with equation (4.10). The influence is calculated at a point $P(x, y, z)$ as shown in the figure (4.3). The point $P(x, y, z)$ is transformed in the panel local coordinates along with the panel corner points.

$$\phi = \frac{-1}{4\pi} \sum_{panel\ edges} \left\{ \left[\frac{(x - x_a)(y_b - y_a) - (y - y_a)(x_b - x_a)}{d_{ab}} \log \frac{r_a + r_b + d_{ab}}{r_a + r_b - d_{ab}} \right] - z \left[tan^{-1} \left(\frac{m_{ab} e_a - h_a}{z r_a} \right) - tan^{-1} \left(\frac{m_{ab} e_b - h_b}{z r_b} \right) \right] \right\} \tag{4.10}$$

where a and b takes the different values of the corners depending on the panel geometry. For a quadrilateral panel:

$$\begin{aligned} edge_1 : &\quad a = 1,\ b = 2 \\ edge_2 : &\quad a = 2,\ b = 3 \\ edge_3 : &\quad a = 3,\ b = 4 \\ edge_4 : &\quad a = 4,\ b = 1 \end{aligned}$$

and other notations used are:

$$\begin{aligned} d_{ab} &= \sqrt{(x_b - x_1)^2 + (y_b - y_a)^2} \\ r_a &= \sqrt{(x - x_a)^2 + (y - y_a)^2 + z^2} \\ r_b &= \sqrt{(x - x_b)^2 + (y - y_b)^2 + z^2} \\ m_{ab} &= \frac{y_b - y_a}{x_b - x_a} \\ e_a &= (x - x_a)^2 + z^2 \\ e_b &= (x - x_b)^2 + z^2 \\ h_a &= (x - x_a)(y - y_a) \\ h_b &= (x - x_b)(y - y_b) \end{aligned}$$

Care must be taken while implementing above formula and various checks needs to be implemented to avoid division by zero and avoid getting ∞ for arctan values. If the distance between $\mathbf{x}_{cp}$ and point P is greater than farfield distance computed by equation (4.6), then the influence of the panel can be approximated with point source and is computed by

$$\phi = \frac{-A}{4\pi\sqrt{(x-x_0)^2+(y-y_0)^2+z^2}} \tag{4.11}$$

where $\mathbf{x}_{cp} = (x_0, y_0, 0)$, and A is the panel area.

4.6.2 Influence Coefficient due to Doublet Panel

Similarly, the integral in equation (2.24) for unit doublet strength in the z direction is approximated as

$$\phi = \frac{1}{4\pi}\sum_{panel\ edges}\left[tan^{-1}\left(\frac{m_{ab}e_a - h_a}{zr_a}\right) - tan^{-1}\left(\frac{m_{ab}e_b - h_b}{zr_b}\right)\right] \tag{4.12}$$

$$\text{As } z \to 0, \quad \phi = \mp\frac{1}{2} \tag{4.13}$$

The notations are same as that are used in equation (4.10). The influence of panel on itself is -0.5. If the distance between point of influence and panel collocation point is larger than farfield distance, following approximation can be used:

$$\phi = \frac{-A\ z}{4\pi\left[(x-x_0)^2+(y-y_0)^2+z^2\right]^{3/2}} \tag{4.14}$$

4.7 Calculation of Disturbance Velocity

The disturbance velocity calculations due to constant strength source and doublet panel are described in this section. The induced velocity can be obtained by differentiating the velocity potential formulas. Again Hess and Smith's formulation is employed in the current work. The point $P(x, y, z)$ is transformed in the panel's local coordinates. All velocity formulations in this sections calcu-

lates velocity in the panel's local coordinates and hence the final velocity needs to be transformed in the global coordinates.

4.7.1 Disturbance velocity due to Source Panel

The velocity components for a constant unit strength source panel are:

$$u = \frac{1}{4\pi} \sum_{panel\ edges} \left[\frac{y_b - y_a}{d_{ab}} \log \frac{r_a + r_b - d_{ab}}{r_a + r_b + d_{ab}} \right] \tag{4.15}$$

$$v = \frac{1}{4\pi} \sum_{panel\ edges} \left[\frac{x_a - x_b}{d_{ab}} \log \frac{r_a + r_b - d_{ab}}{r_a + r_b + d_{ab}} \right] \tag{4.16}$$

$$w = \frac{1}{4\pi} \sum_{panel\ edges} \left[tan^{-1} \left(\frac{m_{ab} e_a - h_a}{z r_a} \right) - tan^{-1} \left(\frac{m_{ab} e_b - h_b}{z r_b} \right) \right] \tag{4.17}$$

The u and v components of the velocity are defined everywhere, but at the edges of the quadrilateral they become infinite. In practice, usually the influence of the element on itself is sought, and near the centroid, u and v velocity components approach zero and w approaches ± 0.5. Also if $z \to \pm 0$ and point P lies outside the panel then $w = 0$. If the point P is at a distance greater than farfield distance, then following approximations can be employed:

$$u = \frac{A\ (x - x_0)}{4\pi[(x - x_0)^2 + (y - y_0)^2 + z^2]^{3/2}} \tag{4.18}$$

$$v = \frac{A\ (y - y_0)}{4\pi[(x - x_0)^2 + (y - y_0)^2 + z^2]^{3/2}} \tag{4.19}$$

$$w = \frac{A\ (z - z_0)}{4\pi[(x - x_0)^2 + (y - y_0)^2 + z^2]^{3/2}} \tag{4.20}$$

4.7.2 Disturbance velocity due to Doublet Panel

Doublet panels usually represents body panels and wake panels. Body panels (in most cases) stays planer as there less/no deformation of the body. This is not the case with the wake panels. As time progresses, wake panels are deformed and twisted due to wake roll up and may not remain planar. As shown in [1], constant strength doublet element can be replaced with constant strength vortex ring placed at the panel edges. This vortex ring equivalent of the doublet

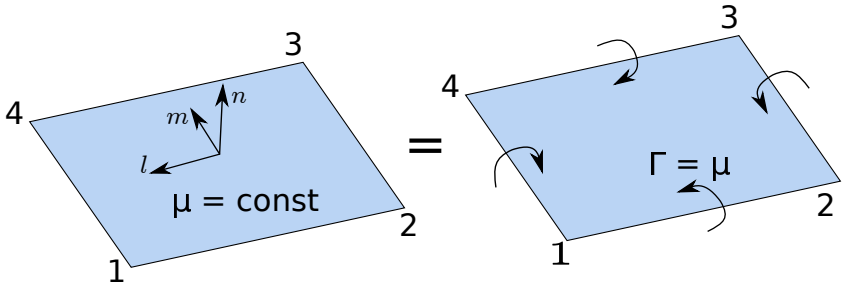

Figure 4.4. Constant strength doublet panel and its equivalent vortex ring element

panel provides more accurate results and can be used on twisted panel as well. Hence the velocity induced due to doublet panel at a point can be found out by summing the velocity due to vortex line elements which are represented by panel edges. The velocity induced by a vortex element is given by Biot-Savart law

$$\Delta \mathbf{u} = \frac{\Gamma}{4\pi} \frac{d\mathbf{l} \times \mathbf{r}}{r^3} \tag{4.21}$$

If the unit strength vortex segment points from point 1 to point 2, then the velocity at arbitrary point $P(x, y, z)$ can be obtained by

$$\mathbf{u}_{1,2} = \frac{1}{4\pi} \frac{\mathbf{r}_1 \times \mathbf{r}_2}{|\mathbf{r}_1 \times \mathbf{r}_2|^2} \left(\frac{\mathbf{r}_0 \,.\, \mathbf{r}_1}{r_1} - \frac{\mathbf{r}_0 \,.\, \mathbf{r}_2}{r_2} \right) \tag{4.22}$$

where

$$\mathbf{r}_1 = \mathbf{x}_P - \mathbf{x}_1$$
$$\mathbf{r}_2 = \mathbf{x}_P - \mathbf{x}_2$$
$$\mathbf{r}_0 = \mathbf{x}_2 - \mathbf{x}_1$$

Similarly, the velocity due to remaining edges is calculated and summed up to get the total velocity of the panel. For calculations of velocity using vortex ring formulation, we do not need to transform the panel coordinates and point P in panel's coordinate, hence the resulting velocity is in the global coordinates (unlike velocity due to source panel).

4.8 Calculation of Surface Velocity

The benefit of using constant strength source and doublet panel method is that the local panel velocity can be obtained locally by differentiating μ over surface, i.e. the disturbance velocity on surface in terms of doublet strength is given by equation (3.23). As an unstructured grid formulation is adopted in the current work, the gradients in (3.23) cannot be evaluated by simple finite difference approximations. We've employed a Least-Square approach [3] to compute the surface velocity. The least-squares approach is based upon the use of a first-order Tayler series approximations. The change of solution along the panel coordinates can be computed from

$$(\nabla \mu_i) . \mathbf{r}_{ij} = \mu_j - \mu_i \tag{4.23}$$

where, the counter i is panel counter and j is the panel's neighbour counter. $\mathbf{r}_{ij} = \mathbf{x}_j - \mathbf{x}_i$ and $\mathbf{x}$ is the panel's collocation point. And μ is the doublet strength of the panel. In matrix form

$$\begin{bmatrix} \Delta x_{i1} & \Delta y_{i1} \\ \Delta x_{i2} & \Delta y_{i2} \\ \vdots & \vdots \\ \Delta x_{iN_A} & \Delta y_{iN_A} \end{bmatrix} \begin{bmatrix} \dfrac{\partial \mu}{\partial l} \\ \dfrac{\partial \mu}{\partial m} \end{bmatrix}_i = \begin{bmatrix} \mu_1 - \mu_i \\ \mu_2 - \mu_i \\ \vdots \\ \mu_{N_A} - \mu_i \end{bmatrix} \tag{4.24}$$

where, N_A is the number of adjacent panels to panel i. Number of adjacent panels are usually 3 or 4. The equation (4.24) is solved using LAPACK's *dgelsd* subroutine. The solution gives the surface velocity in the panel's coordinates. And the velocity in the normal direction will be zero. This disturbance velocity is substituted in equation (3.23) to get the total surface velocity. Again this velocity can be transformed back to global coordinates for visualization.

Chapter 5

Results

This section compares the results of the developed code with the established analytical or experimental results.

5.1 Case 1: Flow over Cylinder

In mathematics, potential flow around a circular cylinder is a classical solution for the flow of an inviscid, incompressible fluid around a cylinder that is transverse to the flow. Far from the cylinder, the flow is unidirectional and uniform. The flow has no vorticity and thus the velocity field is irrotational and can be modeled as a potential flow. Unlike a real fluid, this solution indicates a net zero drag on the body. The analytical solution of the flow over two dimensional cylinder exists and the coefficient of pressure on the cylinder is given by

$$C_p = 1 - 4sin^2(\theta) \tag{5.1}$$

In the present work, a cylinder of $D/L = 1/20$ is used and the coefficient of pressure is shown in the figure (5.1). And figure (5.2) compares the analytical solution with that of developed vortex panel code and can be seen that the solution matches with good accuracy. The flow is at zero degree angle of attack.

When a body moves in a fluid, some amount of fluid must move around it. When the body accelerates, so too must the fluid. Thus, more force is required to accelerate the body in the fluid than in a vacuum. Since force equals mass

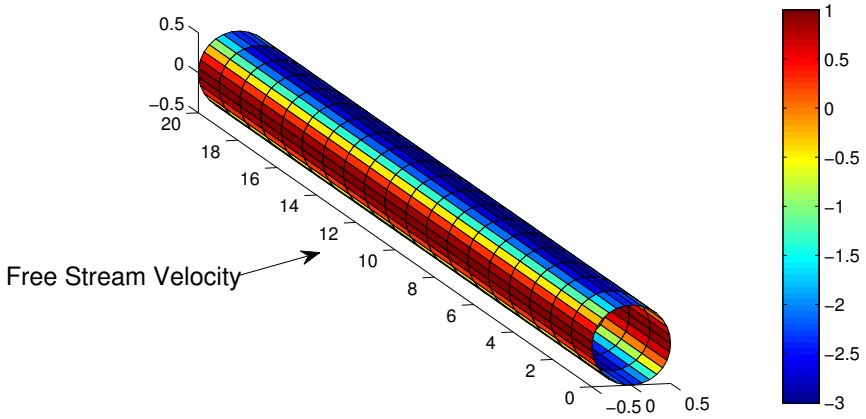

Figure 5.1. Coefficient of pressure on cylinder surface using Vortex Panel Method

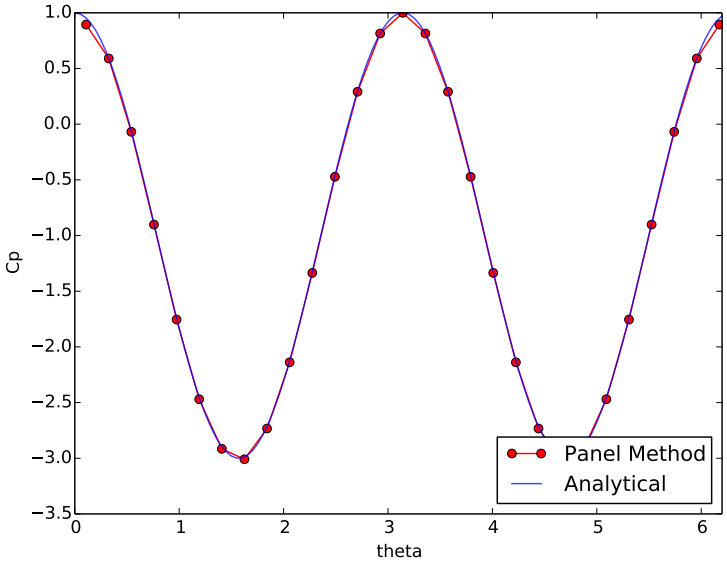

Figure 5.2. Comparison of analytical and numerical solution for flow over cylinder

times acceleration, we can think of the additional force in terms of an imaginary added mass of the object in the fluid. To check the unsteady version of code, it is tested with accelerating cylinder in a stationery fluid and results are compared for added mass of the cylinder. The added mass of a cylinder can be computed

analytically by

$$m_a = \rho \pi r^2 L \tag{5.2}$$

where ρ is the fluid density, r and L are radius and length of the cylinder. And the added mass can be computed using vortex panel method by

$$m_a = \frac{Drag\ force}{Acceleration} \tag{5.3}$$

The added mass of a cylinder of varying length and for an acceleration of 1.5 is calculated and tabulated in the table (5.1) below. It can be seen that the added mass calculated by vortex panel method matches significantly when the aspect ratio of the cylinder is increased.

Table 5.1. Comparison of numerical and analytical Added mass for cylinder.

Cylinder Config.	Panel Method	Analytical	Error(%)
D = 1, L = 5	4.3698	4.8105	9.168
D = 1, L = 10	9.3244	9.6211	3.083
D = 1, L = 15	14.2942	14.4317	0.9527
D = 1, L = 20	19.2699	19.2422	0.1439

5.2 Case 2: NACA0012 Airfoil

NACA0012 airfoil is used for wide range of applications such as aircraft, helicopter blades etc. and also wide range of experimental results are available for this airfoil. Thus this makes an ideal test case to validate the results. The figures (5.3) and (5.4) shows the coefficient of pressure at 0 and 10 degree angle of attack, respectively and are compared with the experimental results [6]. As the airfoil is symmetric, the pressure on upper and lower surfaces at $\alpha = 0^o$ is same. For $\alpha = 10$, pressure on upper surface is only available in experimental results. The variation of the coefficient of lift with angle of attach (α) is plotted in the figure (5.5).

Also two unsteady motions of the NACA0012 airfoil are studied. The first case is when naca airfoil is suddenly kept in an uniform motion (starting from

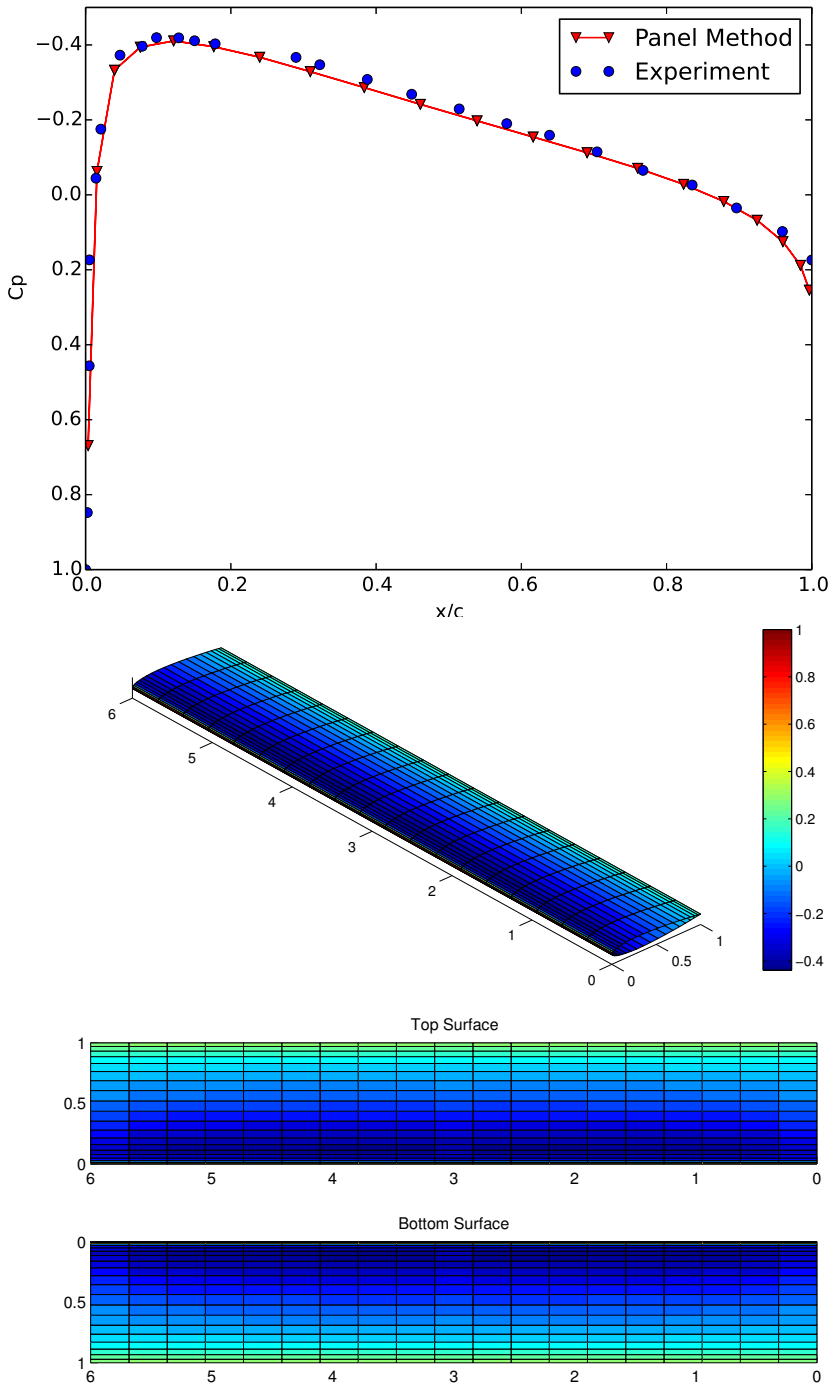

Figure 5.3. Coefficient of pressure on NACA0012 airfoil at 0^o angle of attack.

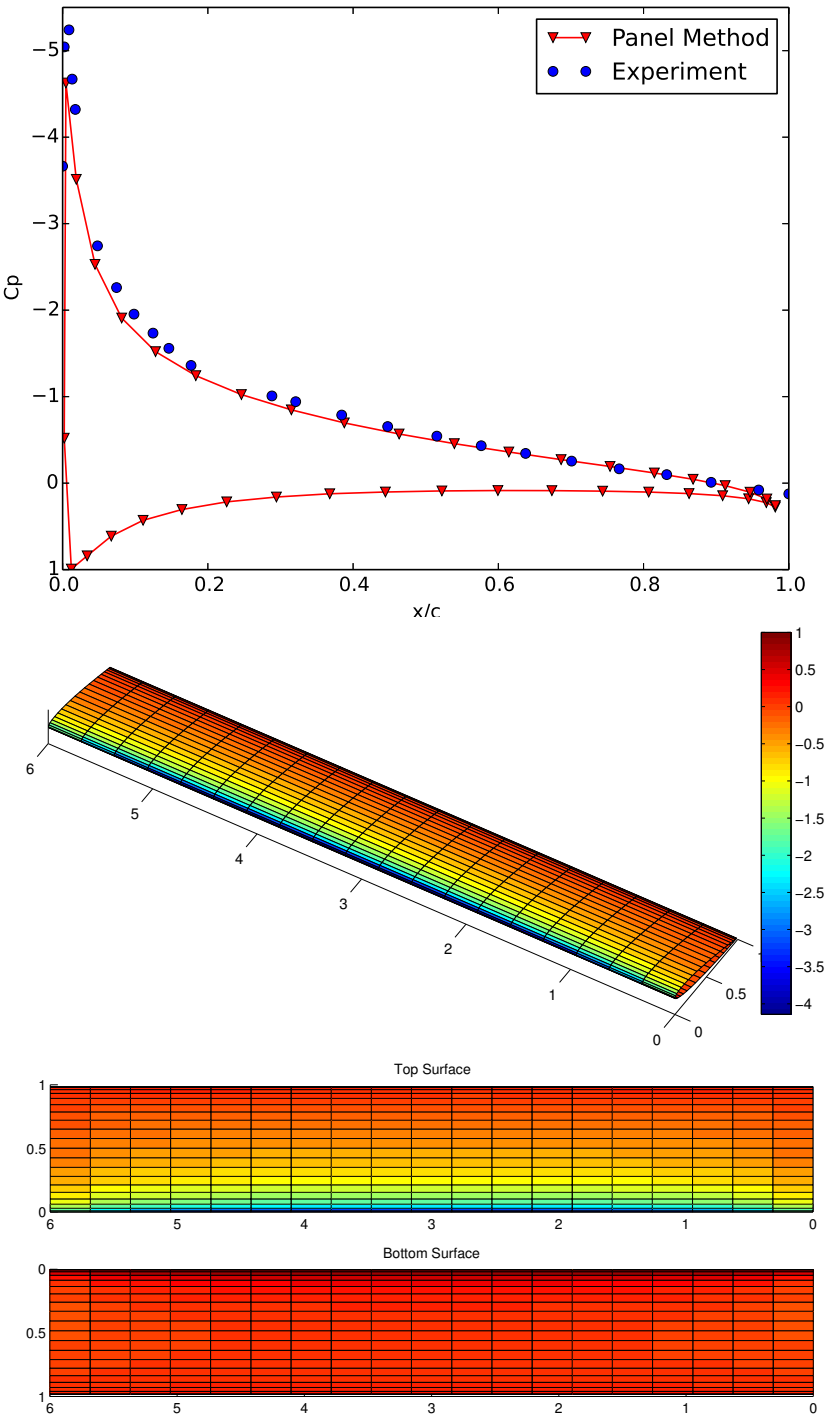

Figure 5.4. Coefficient of pressure on NACA0012 airfoil at 10^o angle of attack.

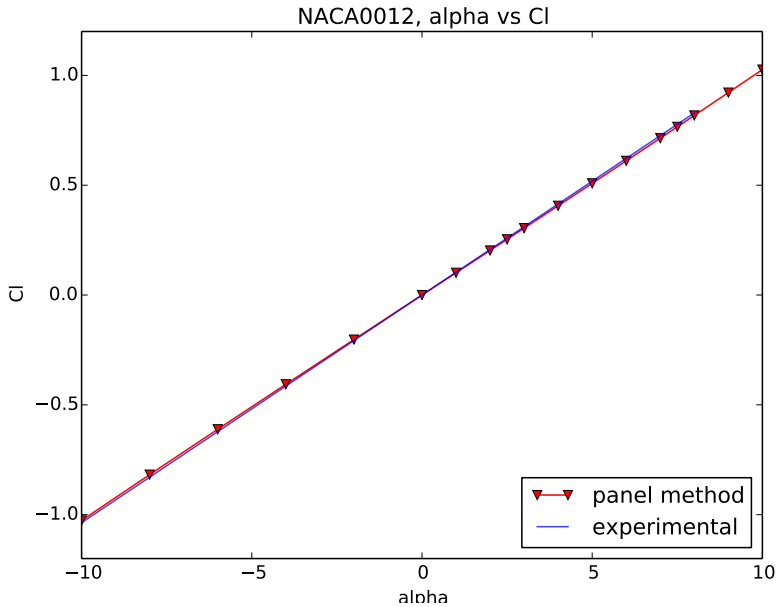

Figure 5.5. Variation of coefficient of lift with respect to α.

rest). Here the airfoil makes an angle of attack of 10^0. The shape of the wake gives us a fair idea how the flow field in the wake is as wake is allowed to move with the local induced velocity (wake-rollup). The solution of pressure distribution achieves the steady state solution after few iterations.

The figure (5.6) shows the free wake developed behind the naca airfoil. The

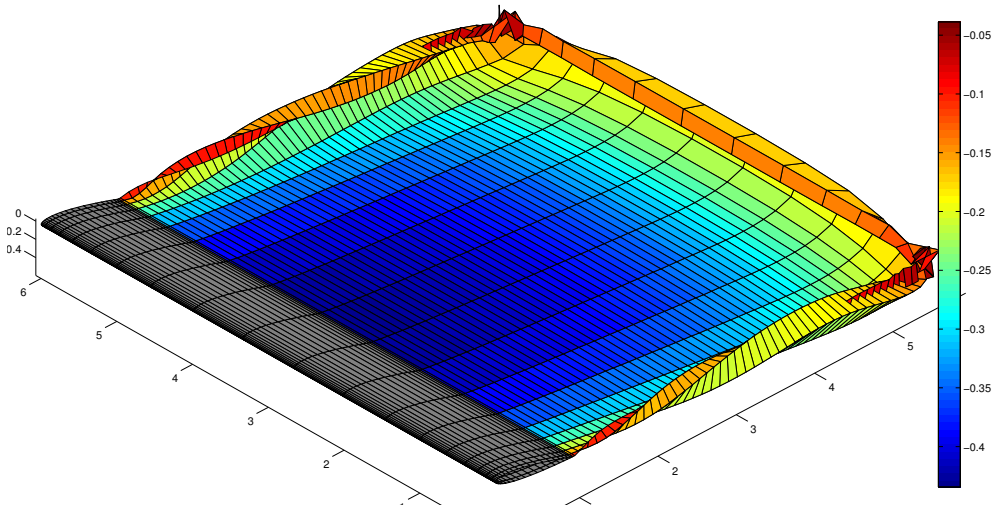

Figure 5.6. Free wake behind naca0012 airfoil when suddenly kept in uniform motion at $\alpha = 10^o$. The wake is coloured with the wake panel (doublet) strengths.

Figure 5.7. Starting vortex behind naca0012 airfoil when suddenly kept in uniform motion at $\alpha = 10^o$.

tip vortex generated can be easily seen as the wake itself is twisted at tip of the airfoil. Also the starting vortex can be observed. The figure (5.7) shows the cross-section of the airfoil at the midplane to visualise the starting vortex.

The second case simulates the heaving motion of the naca0012 airfoil in an uniform flow. The various parameters to define the heaving problem as follows:

$$\begin{aligned} \mathbf{U}_\infty &= \left(0.009\,\frac{chord\ length}{\Delta t},\ 0,\ 0\right) \\ Amplitude_{max} &= 0.019\,chord\ length \\ Reduced\ frequence\ (k) &= 8.57 \\ \omega &= 2\,k\,U_\infty / chord\ length \\ \mathbf{v}_{body} &= (0,\ 0,\ Amplitude_{max}\,cos(\omega t)) \end{aligned}$$

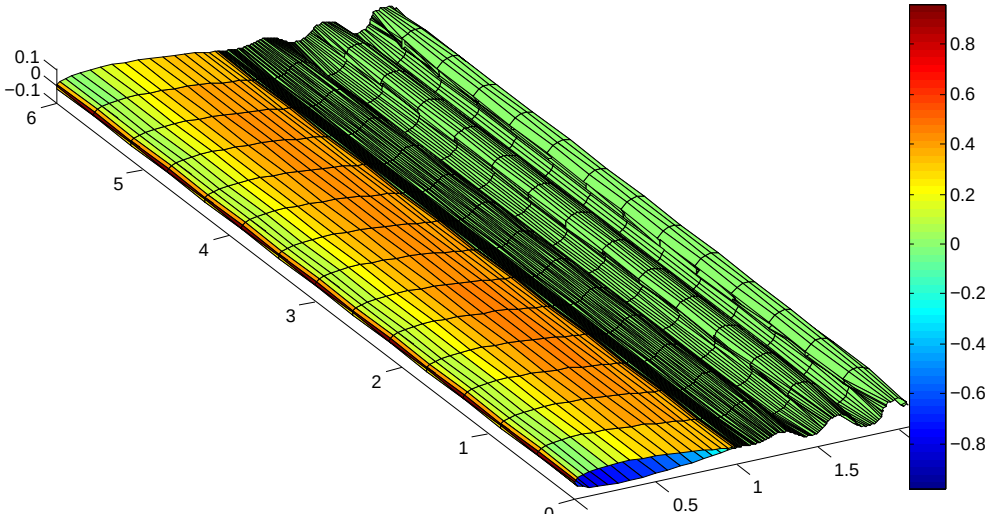

Figure 5.8. Heaving motion of the naca0012 airfoil. The airfoil is coloured with instantaneous pressure coefficient

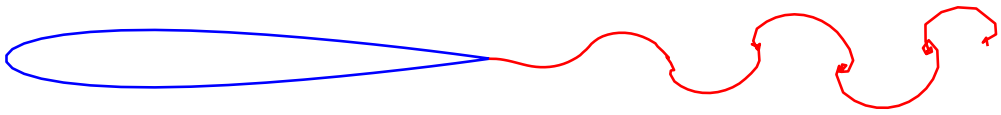

Figure 5.9. Wake developed behind naca0012 airfoil in heaving motion.

where the chord length of the airfoil used is $1m$ and time step (Δt) is 0.025. $\mathbf{U}_\infty$ is free stream velocity which is constant throughout, $Amplitude_{max}$ is the maximum heaving amplitude, ω is the heaving frequency, $\mathbf{v}_{body}$ is instantaneous velocity of the body and t is the time.

5.3 Case 3: NREL Phase-VI Wind Turbine Experiments

The National Renewable Energy Laboratory (NREL) conducted a series of wind tunnel experiments on wind turbine to study the 3D unsteady aerodynamics of the wind turbine blades. The wind turbine blade uses S809 airfoil which is a thick airfoil and panel method is an ideal candidate for calculating flow over thick bodies. Though the airfoil used in the wind turbine blade is same, its chord length and twist angle is varying along the span. The details of the blade geometry can be found in [7]. From the various sequence of tests conducted by NREL, sequence S is used to validate the panel method code for a varying 3D geometry. From this sequence a case of free stream velocity of $7m/s$ is simulated in the current work. The blade is rotated at 71.63 rpm, the blade tip pitch angle is set to 3^o and the free stream velocity is in upwind direction.

Figures (5.10) and (5.11) plots the coefficient of pressure on blade cross sections at different span stations where experimental results are available. The results of the panel method are in good agreement with the experimental data. The figure (5.12) shows coefficient of pressure over entire blade geometry. The figure (5.13) shows the wake developed behind the blade after 1.5 rotation of the blade.

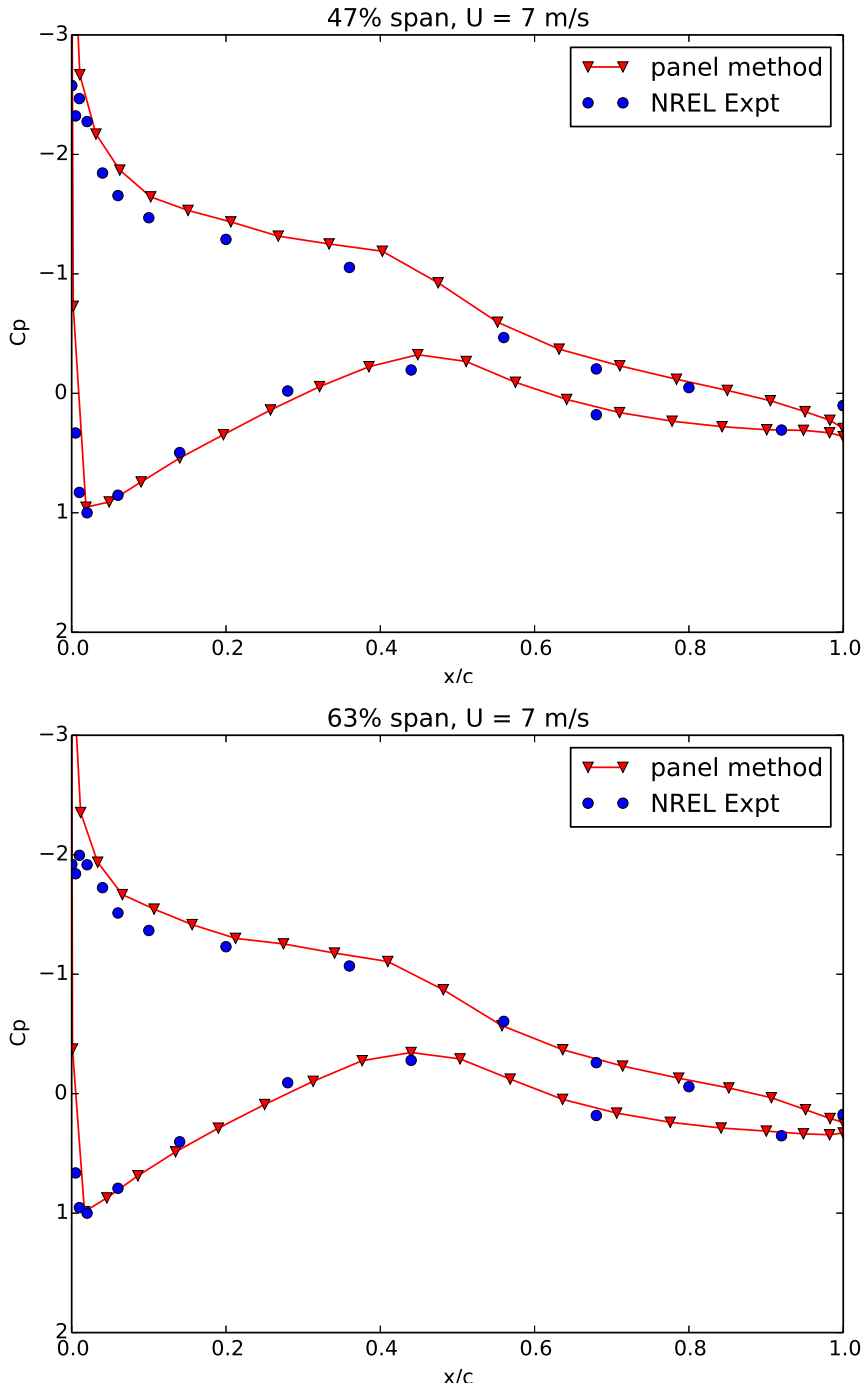

Figure 5.10. Coefficient of pressure on wind turbine blade at 47% and 63% span stations.

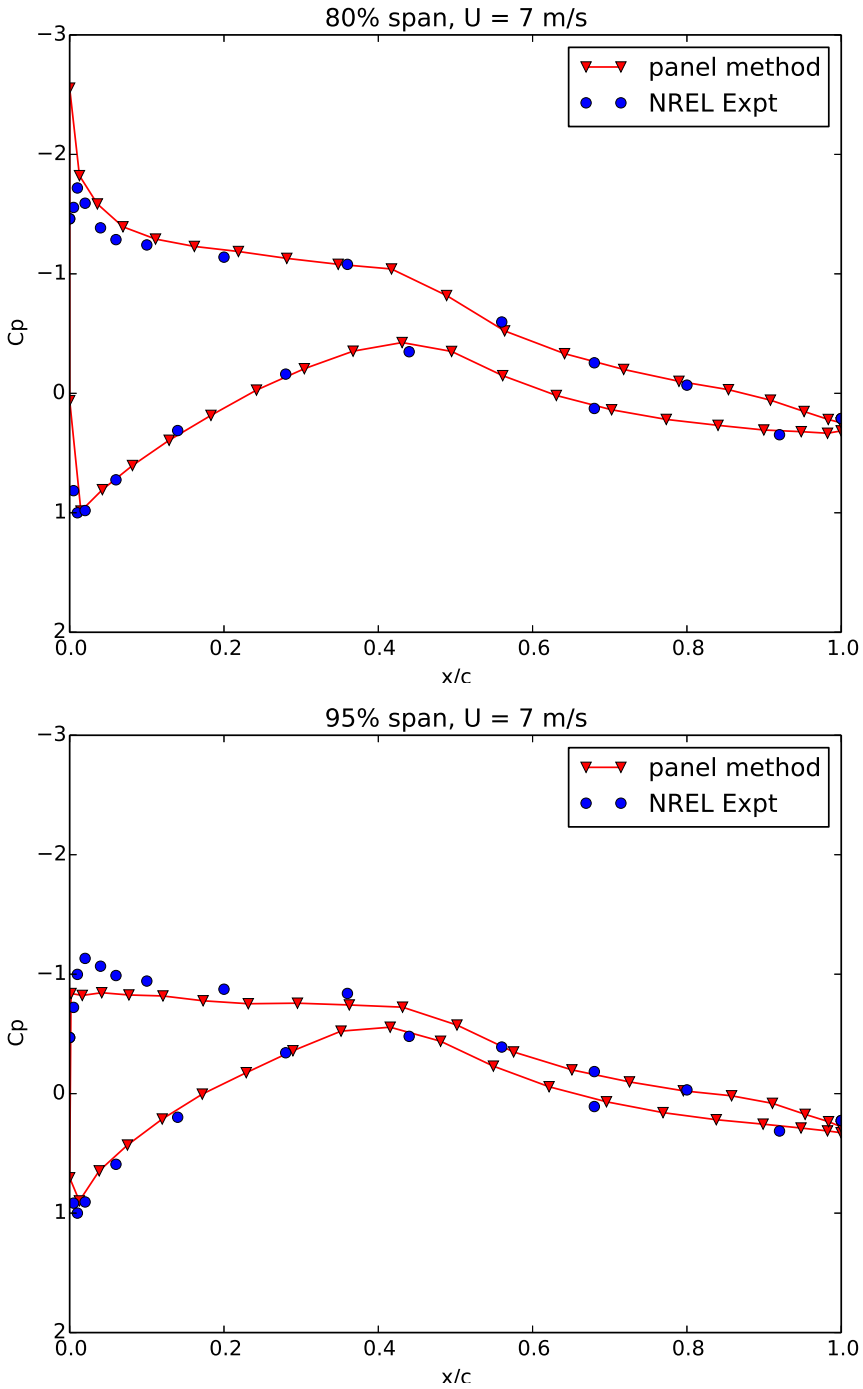

Figure 5.11. Coefficient of pressure on wind turbine blade at 80% and 95% span stations.

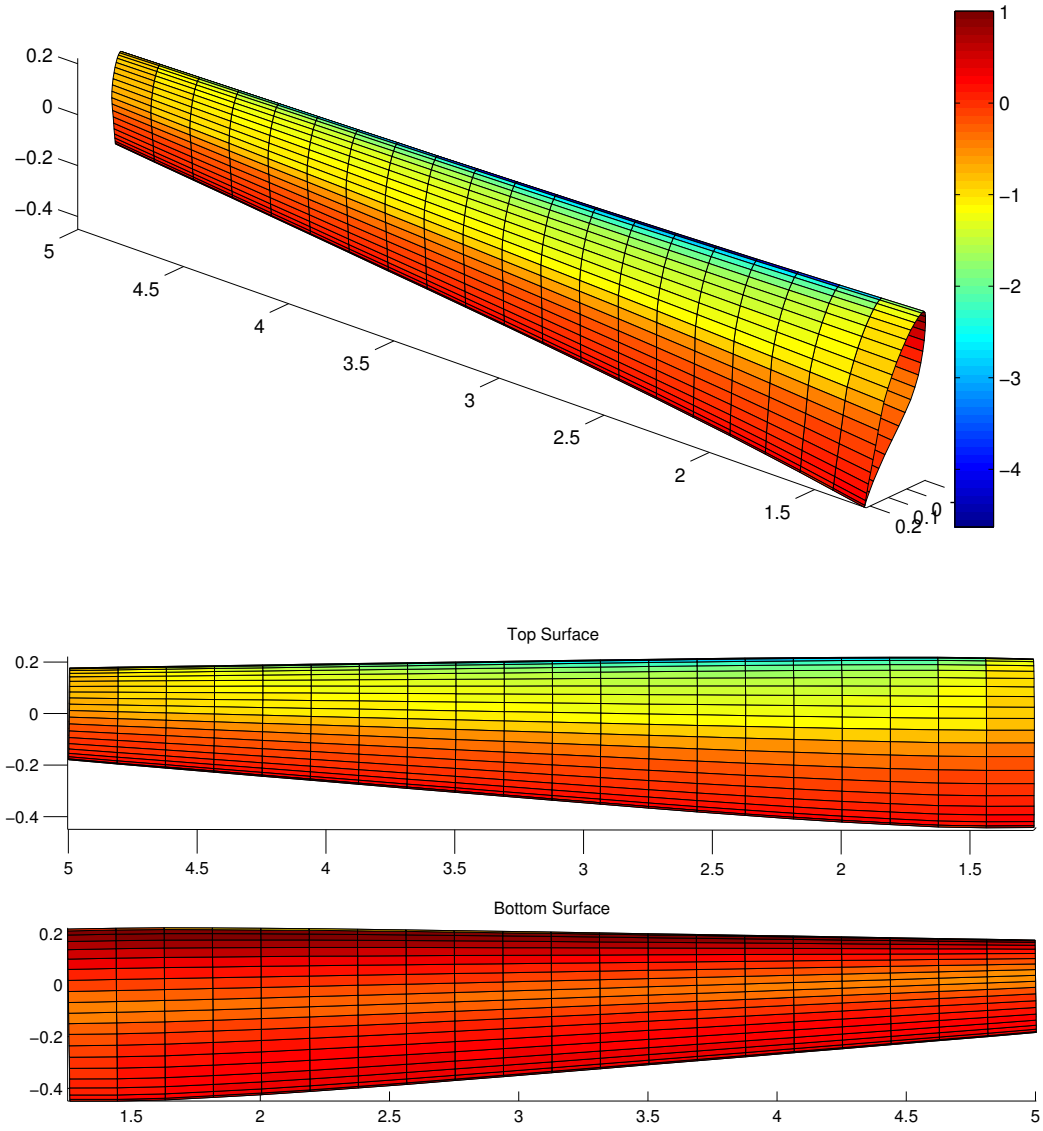

Figure 5.12. Coefficient of pressure on wind turbine blade.

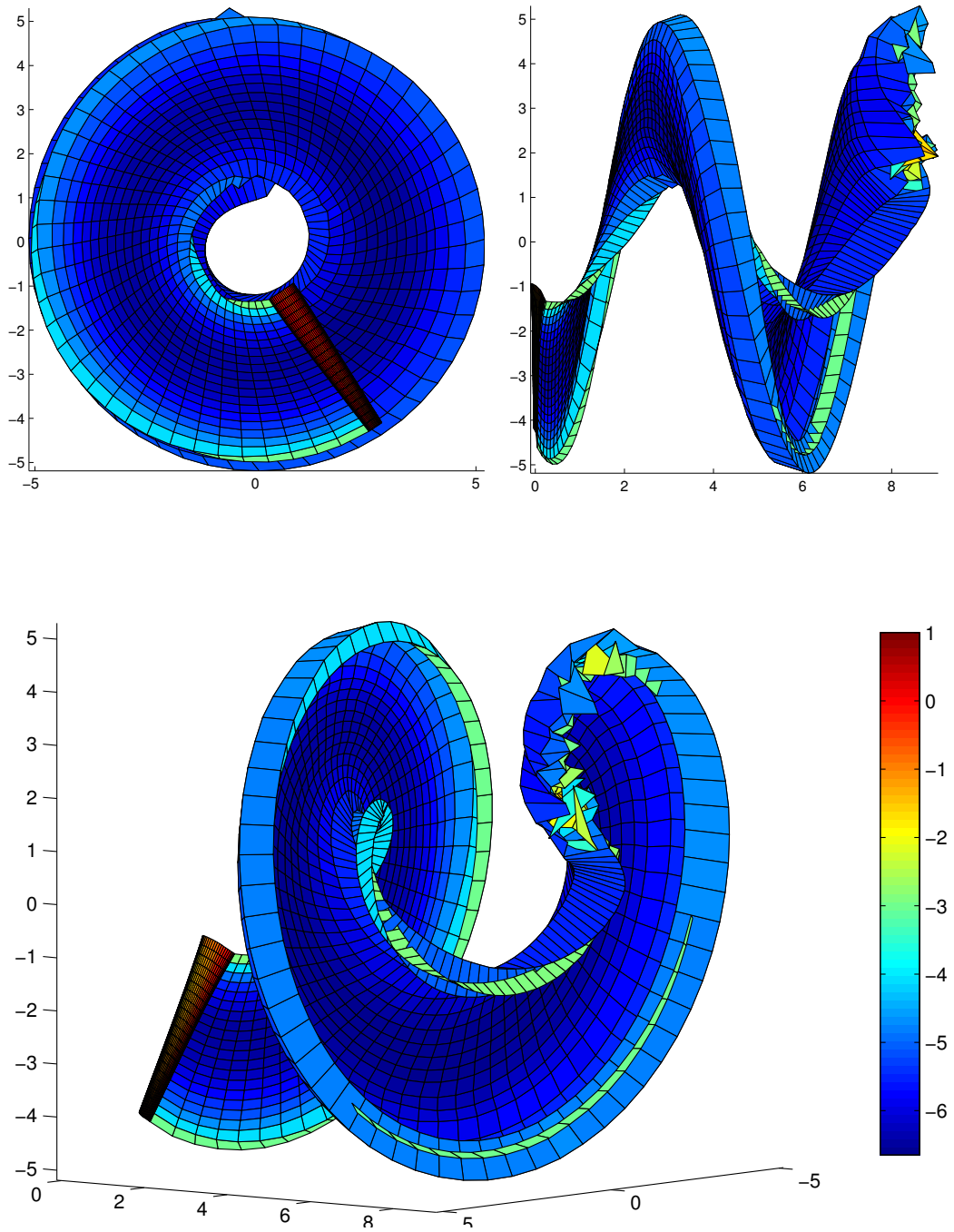

Figure 5.13. Wake behind the wind turbine after 1.5 blade rotation. The wake is coloured by strength the wake (doublet) panels.

Chapter 6

Conclusion and Future work

In the current work a three dimensional unsteady vortex panel method is developed. And it is successfully validated by comparing its solution with various analytical and experimental results. It can be concluded that vortex panel method is an ideal method to use for computing flow over an object when there is no separation and effects of viscosity are less.

The solution for flow over cylinder matched with the analytical solution and also the added mass of cylinder came in agreement with the analytical added mass of the cylinder. This provides the validation of the unsteady panel method which is developed for current work. Also the flow over NACA0012 airfoil is studied and solution found to be in agreement with experimental results. Force free wake model has been implemented to capture the unsteady flow behaviour.

The current developed method solves for a potential flow around a body and neglects any viscous effects. However for a real flow, the viscous effects should be considered to get more realistic situations. Along with potential flow, boundary equations can be coupled with the potential flow solution to take into account for the viscous effects. Laminar, transition and also turbulent boundary layers can be taken into account.

Bibliography

[1] J. Katz and A. Plotkin, ***Low Speed Aerodynamics, Second Edition***, Cambridge University Press.

[2] Hess, J. L., and Smith, A. M. O., ***Calculation of Potential Flow About Arbitrary Bodies***, Progress in Aeronautical Sciences, Vol. 8, 1967, pp. 1138.

[3] J. Blazek, ***Computational Fluid Dynamics: Principles and Applications***, Elsevier 2001

[4] Ashby, L. D., Dudley, M. D., Iguchi, S. K., Browne, L., and Katz, J., ***Potential Flow Theory and Operation Guide for the Panel Code PMARC***, NASA TM 102851, March 1990.

[5] Lamb, H., ***Hydrodynamics***, Dover, 6th edition, 1945

[6] Turbulence Modeling Resource, Langley Research Center. (`http://turbmodels.larc.nasa.gov/naca0012_val.html`)

[7] M.M. Hand, D.A. Simms, L.J. Fingersh, D.W. Jager, J.R. Cotrell, S. Schreck, and S.M. Larwood, ***Unsteady Aerodynamics Experiment Phase VI: Wind Tunnel Test Configurations and Available Data Campaigns***, National Renewable Energy Laboratory